

# Gut commensal *Parabacteroides goldsteinii* plays a predominant role in the anti-obesity effects of polysaccharides isolated from *Hirsutella sinensis*

Tsung-Ru Wu,<sup>1,2</sup> Chuan-Sheng Lin,<sup>1,3,4,5,6</sup> Chih-Jung Chang,<sup>1,3,4,5,6</sup> Tzu-Lung Lin,<sup>1</sup> Jan Martel,<sup>3,5</sup> Yun-Fei Ko,<sup>5,7,8</sup> David M Ojcius,<sup>3,5,9</sup> Chia-Chen Lu,<sup>10</sup> John D Young,<sup>3,5,7,8,11</sup> Hsin-Chih Lai<sup>1,3,4,5,6,12,13,14</sup>

► Additional material is published online only. To view, please visit the journal online (<http://dx.doi.org/10.1136/gutjnl-2017-315458>).

For numbered affiliations see end of article.

## Correspondence to

Dr John D Young, Center for Molecular and Clinical Immunology, Chang Gung University, Gueishan, Taoyuan 33302, Taiwan; [jdyoung@mail.cgu.edu.tw](mailto:jdyoung@mail.cgu.edu.tw) and Dr Hsin-Chih Lai, Department of Medical Biotechnology and Laboratory Science, College of Medicine, Chang Gung University, Gueishan, Taoyuan 33302, Taiwan; [hclai@mail.cgu.edu.tw](mailto:hclai@mail.cgu.edu.tw)

T-RW, C-SL and C-JC contributed equally.

Received 13 October 2017

Revised 22 June 2018

Accepted 22 June 2018

Published Online First

14 July 2018



© Author(s) (or their employer(s)) 2019. No commercial re-use. See rights and permissions. Published by BMJ.

**To cite:** Wu T-R, Lin C-S, Chang C-J, et al. *Gut* 2019;**68**:248–262.

## ABSTRACT

**Objective** The medicinal fungus *Ophiocordyceps sinensis* and its anamorph *Hirsutella sinensis* have a long history of use in traditional Chinese medicine for their immunomodulatory properties. Alterations of the gut microbiota have been described in obesity and type 2 diabetes. We examined the possibility that *H. sinensis* mycelium (HSM) and isolated fractions containing polysaccharides may prevent diet-induced obesity and type 2 diabetes by modulating the composition of the gut microbiota.

**Design** High-fat diet (HFD)-fed mice were treated with HSM or fractions containing polysaccharides of different molecular weights. The effects of HSM and polysaccharides on the gut microbiota were assessed by horizontal faecal microbiota transplantation (FMT), antibiotic treatment and 16S rDNA-based microbiota analysis.

**Results** Fraction H1 containing high-molecular weight polysaccharides (>300 kDa) considerably reduced body weight gain (~50% reduction) and metabolic disorders in HFD-fed mice. These effects were associated with increased expression of thermogenesis protein markers in adipose tissues, enhanced gut integrity, reduced intestinal and systemic inflammation and improved insulin sensitivity and lipid metabolism. Gut microbiota analysis revealed that H1 polysaccharides selectively promoted the growth of *Parabacteroides goldsteinii*, a commensal bacterium whose level was reduced in HFD-fed mice. FMT combined with antibiotic treatment showed that neomycin-sensitive gut bacteria negatively correlated with obesity traits and were required for H1's anti-obesogenic effects. Notably, oral treatment of HFD-fed mice with live *P. goldsteinii* reduced obesity and was associated with increased adipose tissue thermogenesis, enhanced intestinal integrity and reduced levels of inflammation and insulin resistance.

**Conclusions** HSM polysaccharides and the gut bacterium *P. goldsteinii* represent novel prebiotics and probiotics that may be used to treat obesity and type 2 diabetes.

## INTRODUCTION

Obesity is a metabolic disorder associated with increased risk of developing type 2 diabetes mellitus, cardiovascular disease and cancer.<sup>1–4</sup> Obesity is

## Significance of this study

### What is already known on this subject?

- Diet-induced dysbiosis and leaky gut contribute to the development of obesity and type 2 diabetes.
- Polysaccharides derived from medicinal fungi such as *Ganoderma lucidum* reduce weight gain in obese mice.
- *Hirsutella sinensis* mycelium (HSM) produces anti-inflammatory, hypoglycaemic and lipid-lowering effects in animals.

### What are the new findings?

- High-molecular weight polysaccharides (>300 kDa) derived from HSM produce anti-obesogenic and antidiabetic effects in obese mice.
- HSM polysaccharides reverse obesity-induced gut dysbiosis and leaky gut, and reduce metabolic endotoxemia, inflammation, insulin resistance and dyslipidemia.
- HSM polysaccharides modulate the composition of the gut microbiota, notably by enriching the gut bacterium *Parabacteroides goldsteinii*.
- Oral treatment of obese mice with live *P. goldsteinii* bacteria prevents body weight gain, improves intestinal integrity and reduces inflammation and insulin resistance.

### How might it impact on clinical practice in the foreseeable future?

- High-molecular weight polysaccharides derived from HSM represent novel prebiotics to treat obesity and type 2 diabetes.
- *P. goldsteinii* is a novel probiotic bacterium that may be used to treat obesity and associated metabolic disorders.

characterised by body weight gain, accumulation of fat tissues, gut microbiota dysbiosis,<sup>5</sup> leaky gut,<sup>6</sup> metabolic endotoxemia,<sup>6,7</sup> chronic inflammation,<sup>6,8</sup> insulin resistance<sup>6,9,10</sup> and adipocyte hypertrophy.<sup>11</sup> Excess body weight also contributes to the development of non-alcoholic fatty liver disease (NAFLD) and non-alcoholic steatohepatitis (NASH).<sup>9</sup>

Recent studies indicate that gut microbiota dysbiosis is associated with disrupted gut barrier function and metabolic endotoxemia.<sup>12–15</sup> Strategies that restore the gut microbiota have thus been proposed to prevent and treat obesity.<sup>16–19</sup> Diet represents a critical factor that affects host metabolism by modulating the gut microbiota.<sup>20</sup> Several studies have shown that modulation of the gut microbiota using prebiotics and probiotics may improve intestinal integrity and host metabolism and reduce obesity and chronic inflammation.<sup>17–21–24</sup> Polysaccharides and dietary fibre can reduce body weight and exert anti-inflammatory effects by enhancing the growth of specific anti-obesogenic gut bacteria and the production of microbiota-derived metabolites.<sup>25–27</sup> However, further studies are needed to better understand the complex interactions between diet, prebiotics and the gut microbiota.

Many herbal remedies used in traditional Chinese medicine (TCM) exert anti-obesogenic and antidiabetic effects.<sup>28</sup> One class of traditional remedies consists of medicinal fungi, such as *Ophiocordyceps sinensis* and *Ganoderma lucidum*, which contain a wide range of immunomodulatory and bioactive compounds.<sup>29–32</sup> We previously observed that *G. lucidum* reduces obesity in high-fat diet (HFD)-fed mice by modulating the composition of the gut microbiota.<sup>33</sup> The caterpillar fungus, *O. sinensis* (also called cordyceps), and its anamorph, *Hirsutella sinensis*, also produce immunomodulatory, anti-inflammatory, hypoglycaemic and lipid-lowering effects,<sup>34–35</sup> but the possibility that this fungus may induce anti-obesogenic effects has not been examined.

In the present study, we show that a water extract of *H. sinensis* mycelium (HSM) and polysaccharide-containing fractions isolated from the extract reduce body weight and accumulation of fat tissues in a murine model of diet-induced obesity. Further experiments showed that neomycin-sensitive bacteria including *Parabacteroides goldsteinii* are required for the anti-obesogenic effects of HSM polysaccharides. Thus, our results reveal the existence of a new commensal bacterial species responsible for the anti-obesogenic effects of fungal polysaccharides.

## METHODS

### Animal experiments

Four-week-old C57BL/6J male mice were purchased from the NARLab facility (Taiwan). Animals were housed four to five individuals per cage with free access to food and sterile drinking water (DW) (reverse osmosis grade) in a temperature-controlled room (21°C±2°C) under a 12 hours dark-light cycle. After an accommodation period of 1 week, mice were fed for 12 weeks with standard chow diet (chow, 13.5% of energy from fat; LabDiet 5001; LabDiet, USA) or HFD (60% of energy from fat; TestDiet 58Y1; TestDiet, USA). Mice were supplemented daily with 100 µL of sterile saline (vehicle), HSM (20 mg/kg) or polysaccharide fractions H1–H4 (20 mg/kg) by intragastric gavage. At the time indicated, non-fasting animals were anaesthetised and whole blood was withdrawn by cardiac puncture. Visceral adipose tissues (ie, epididymal white adipose tissues) and the liver were removed and weighed. Organs and tissues were immersed in liquid nitrogen and stored at –80°C for further analysis.

### Preparation of HSM water extract and polysaccharides

*H. sinensis* strain CGB 999335 was isolated and cultured as described previously.<sup>36</sup> HSM consisted of <10% crude fibre; >3% polysaccharides; crude proteins at 42.8 g/100 g; crude fat at 8.2 g/100 g; carbohydrates at 31.9 g/100 g; amino acids at 7.8 g/100 g and sodium at 242.7 mg/100 g. Calories were

measured at 373 kcal per 100 g. HSM water extract and polysaccharide fractions were prepared as described earlier for *G. lucidum*.<sup>33</sup>

### Measurement of serum cytokines

Whole blood was withdrawn by cardiac puncture in tubes containing no anticoagulant (BD, USA). Blood was allowed to clot for 30 min. Solutions were centrifuged at 15 000 g for 1 min and supernatants (serum) were collected. ELISA kits were used to measure interleukin (IL)-1β and tumour necrosis factor-α (TNF-α) from serum according to the manufacturer's instructions (R&D Systems, USA).

### Serum endotoxin detection

Serum endotoxin was quantified using a *Limulus amaebocyte* lysate (LAL) kit (Cambrex Bio Science, USA) according to the manufacturer's instructions.

Briefly, serum samples were diluted 1:10 to 1:1000 in endotoxin-free water (Lonza, USA), heated at 70°C for 10–15 min and processed according to the manufacturer's protocol. Recovery rate was determined based on the net lipopolysaccharide (LPS) concentration of spiked samples supplemented with LPS (0.1 EU/mL, Sigma, USA). Samples with a recovery rate of at least 50% were considered.

### Measurement of homeostatic model assessment-insulin resistance index

Fasting blood glucose was measured using glucometer strips (Johnson & Johnson Medical Devices, Hong Kong) as done before.<sup>37</sup> Fasting insulin was measured using a commercial ELISA kit (Mercodia, Sweden). Homeostatic model assessment-insulin resistance (HOMA-IR) was calculated using the following equation: fasting glucose (mg/dL) × fasting insulin (µU/mL)/405.

### In vivo intestinal permeability assay

Intestinal permeability was assessed in vivo following oral administration of fluorescein-isothiocyanate (FITC)-dextran (4 kDa; Sigma), a high molecular weight glucose polymer which, based on the information provided by the manufacturer, is neither digested nor absorbed by healthy mice. Animals were orally gavaged with FITC-dextran (44 mg/100 g), 4 hours before sacrifice. Whole blood was obtained by cardiac puncture before killing. Serum was diluted with phosphate-buffered saline (PBS) and fluorescence was monitored using a spectrophotofluorometer (Synergy HT, BioTek, USA) using excitation at 485 nm and emission at 528 nm. A standard curve was prepared based on a series of twofold dilution of FITC-dextran in PBS. Serum from mice that had not received FITC-dextran was used as background control.

### In vitro Caco-2 cell monolayer permeability assay

Human Caco-2 cells were purchased from European Collection of Authenticated Cell Cultures (UK). Caco-2 cells were cultured in Dulbecco's modified Eagle's medium supplemented with 10% fetal bovine serum, 50 U/mL penicillin and streptomycin at 37°C under 5% CO<sub>2</sub>. Caco-2 cells (1 × 10<sup>5</sup>) were grown on polyethylene terephthalate membrane-based transwell plates (0.4 µm pores; Millipore, USA) for 21 days to reach confluence (trans-epithelial electrical resistance (TEER) >1000 Ωcm<sup>2</sup>). Caco-2 monolayer grown on the apical side of transwells were treated with LPS (100 µg/mL; O111:B4, Sigma) and 1 mg/mL of H1 or 50 multiplicity of infection of *P. goldsteinii*. LPS diluted in serum-free medium served as a positive control, and serum-free

medium as vehicle control. TEER values were monitored for 12 hours using a Millicell-ERS-2 volt-ohm metre (Millipore).

### Antibiotic treatment

For in vivo antibiotic treatment, HFD-fed mice were treated with either H1 or saline, combined with 50 µg/mL clindamycin (C) (Goldbio, USA), 50 µg/mL metronidazole (M) (Sigma), 50 µg/mL penicillin (P) (Sigma), 25 µg/mL vancomycin (V) (Sigma) and/or 50 µg/mL neomycin (N) (Sigma) in sterile DW for 12 weeks. For ex vivo faecal microbiota transplantation (FMT), HFD-fed mice (aged 5 weeks, male) were treated daily with H1 or saline by oral gavage for 6 weeks. During week 4 to week 6 (total of 14 days), faecal microbiota from each donor mouse was collected daily, treated with antibiotics, pooled, mixed and stored at -80°C. To prepare faecal microbiota, faeces pellets (150–180 mg) were collected daily in sterile tubes, prior to suspension and homogenisation in 1 mL of PBS. After centrifugation at 2000g at 4°C for 1 min, bacteria-enriched supernatants were collected and centrifuged 5 min at 15 000g. Bacterial pellets were resuspended in 1 mL of sterile saline containing the antibiotics CMPV, neomycin or CMPVN, followed by stationary incubation under aerobic conditions at 37°C for 2 hours. After antibiotic treatment, faecal microbiota specimens were collected, washed twice with saline, resuspended in 700 µL of saline with 20% (v/v) glycerol and stored at -80°C. HFD-fed mice (aged 5 weeks, male) were treated daily with faecal microbiota transplants from each donor group via oral gavage for 12 weeks.

### Caecal microbiota analysis

Caecal microbiota DNA was extracted using the QIAamp DNA Stool Mini Kit (Qiagen, USA) and applied to amplification of V3-V4 regions of 16S rDNA. Caecal microbiota composition was assessed using Illumina HiSeq sequencing of 16S rDNA amplicon and QIIME-based microbiota analysis. The detailed procedure of caecal microbiota DNA extraction, sequencing and library construction and microbiota analysis pipeline is described in the supplementary methods.

### *P. goldsteinii* cultivation, preparation and treatment

*P. goldsteinii* (ATCC BAA-1180, also called JCM 13446) was purchased from the American Type Culture Collection (ATCC, USA). Bacteria were grown at 37°C in a Whitley DG250 anaerobic chamber (Don Whitley, UK) with mixed anaerobic gas (5% carbon dioxide, 5% hydrogen, 90% nitrogen). Anaerobicity was confirmed using an anaerobic indicator (Oxoid, UK). *P. goldsteinii* was cultivated on anaerobic blood agar (Creative, Taiwan) and liquid thioglycollate medium (BD). *P. goldsteinii* was collected by centrifugation and resuspended in sterile saline. Mice were treated daily with  $4 \times 10^7$  colony-forming units of *P. goldsteinii* by oral gavage. Heat-killed or pasteurised *P. goldsteinii* were prepared by heating bacteria at 100°C for 15 min or 70°C for 30 min, respectively. Mice were treated daily with either heat-killed or pasteurised *P. goldsteinii* by oral gavage.

### Statistical analysis

Statistical analysis was performed using GraphPad Prism V.7.0a (GraphPad Software, USA). Data are shown as means±SD and medians±IQR for parametric and non-parametric analysis, respectively. Differences between two groups were assessed using unpaired two-tailed Student's t-test. Data sets involving more than two groups were assessed by one-way analysis of variance (ANOVA) followed by Bonferroni's post hoc test or by the non-parametric Kruskal-Wallis test with Dunn's multiple

comparisons test. Bacterial species with statistically significant difference were assessed using Metastats.<sup>38</sup> Levels of bacterial species showing statistically significant differences in Metastats data were also evaluated using the non-parametric Kruskal-Wallis test with false discovery rate (FDR) correction for multiple testing (<5%).<sup>39</sup> Correlation coefficients between bacterial species and obesity traits were determined using Spearman's correlation analysis. P values <0.05 were considered to be statistically significant. Where indicated in the figure legends, the method described by Benjamini *et al*<sup>39</sup> was also used to evaluate FDR (<5%) for estimated p values.

## RESULTS

### HSM and polysaccharide fractions reduce body weight in HFD-fed mice

To test the effects of HSM on body weight, we fed mice with an HFD for 12 weeks and supplemented the animals' diet with daily administration of HSM water extract or saline as negative control (see online supplementary figure S1A). Compared with the chow diet, mice fed an HFD showed increased body weight, visceral fat mass, liver weight, serum triglycerides and HOMA-IR index values (see online supplementary figure S1B-H). Notably, HSM significantly reduced these obesity traits in a dose-dependent manner (see online supplementary figure S1B-H).

To identify the compounds responsible for HSM's anti-obesogenic effects, we fractionated the HSM water extract into four fractions based on molecular weight (figure 1A and supplementary table S1). Administration of fraction H1, which contained polysaccharides with a molecular weight above 300 kDa (see online supplementary table S1), reduced body weight by ~50% after 12 weeks compared with HFD (figure 1B-D). Fraction H1 also reduced visceral fat and HOMA-IR index in HFD-fed mice, producing effects similar to those observed for the HSM water extract (figure 1E,F). While fraction H4 containing oligosaccharides and carbohydrates of low molecular weight did not affect body weight or obesity traits, fractions H2 (10–300 kDa) and H3 (<10 kDa) reduced visceral fat pad mass, but produced no effect on body weight or HOMA-IR index (figure 1B-F).

### HSM-derived polysaccharides reduce metabolic disorders in HFD-fed mice

HSM and H1 did not affect energy intake (see online supplementary figure S2A) or fat absorption (see online supplementary figure S2B), indicating that these treatments did not modulate appetite or lipid absorption. In addition, HSM and H1 did not affect caecal or colonic production of short-chain fatty acids (SCFAs), such as acetate, propionate or butyrate (see online supplementary figure S3). On the other hand, HSM and H1 reduced serum triglycerides (see online supplementary figure S4A) and gene expression involved in lipolysis, lipid transport and uptake and lipogenesis in adipose and hepatic tissues (see online supplementary figure S4B,C). HSM and H1 enhanced gene expression associated with hepatic β-oxidation, compared with the HFD group (see online supplementary figure S4C, Acsl3). In comparison, fractions H2–H4 affected some but not all lipid metabolism parameters (see online supplementary figure S4).

HSM and H1–H3 treatment reduced fasting glucose compared with HFD, while only HSM and H1 reduced fasting insulin (see online supplementary figure S5A,B). HSM and fractions H1–H3 improved glucose tolerance in the oral glucose tolerance test (see online supplementary figure S5C,D), but



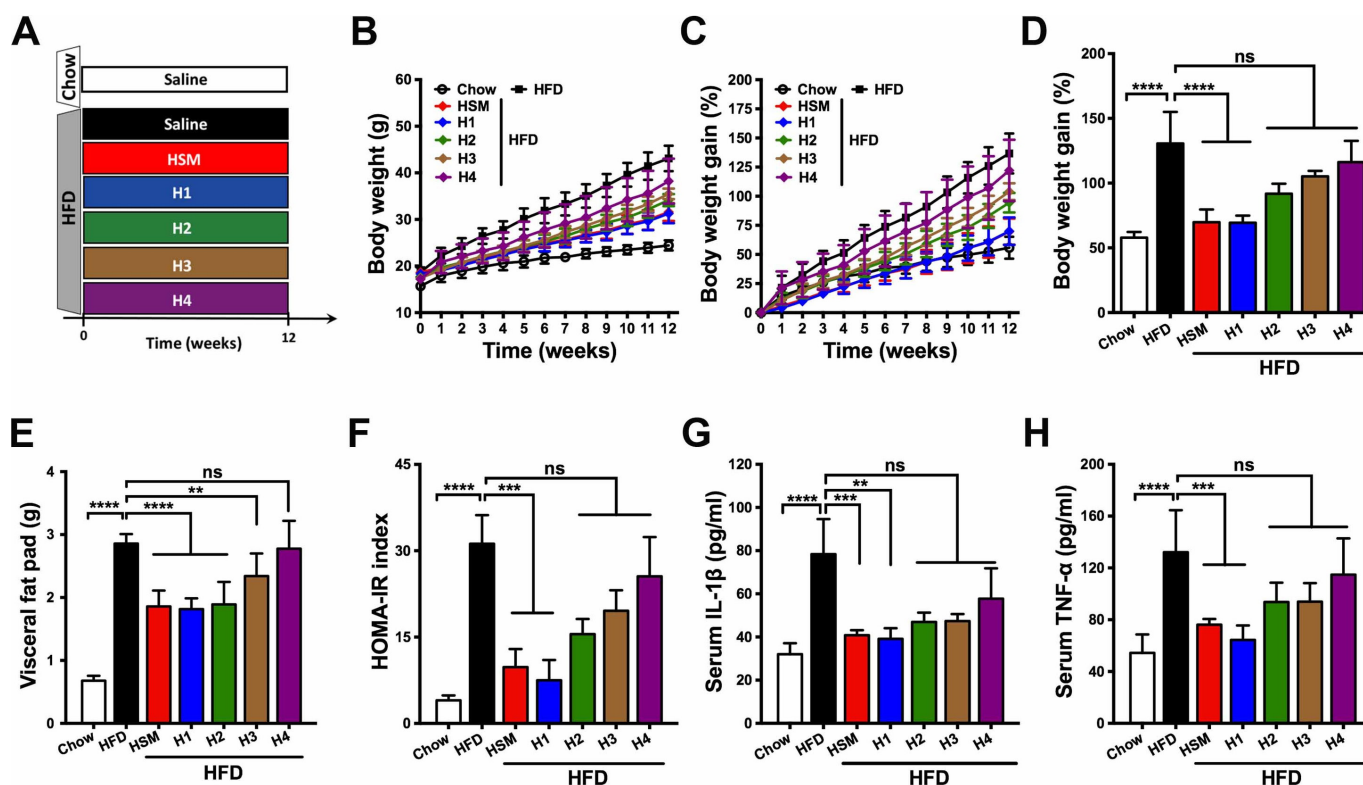


**Figure 1** *Hirsutella sinensis* mycelium (HSM) and H1 reduce diet-induced obesity and metabolic disorders. (A) Chow-fed mice and high-fat diet (HFD)-fed mice were treated daily with control saline, HSM water extract (HSM) (20 mg/kg) or HSM-derived fractions (H1–H4) (20 mg/kg) for 12 weeks by oral gavage. (B) Body weight and (C) relative body weight were measured throughout the 12-week period. Obesity traits including (D) body weight gain, (E) visceral fat pad weight (epididymal white adipose tissue), (F) homeostatic model assessment-insulin resistance (HOMA-IR) index, (G) serum interleukin (IL)-1 $\beta$  and (H) serum tumour necrosis factor- $\alpha$  (TNF- $\alpha$ ) were measured after 12 weeks of treatment as described in the 'Methods' section. Data are presented as means $\pm$ SD from three independent experiments (n=10–15 mice per group). Statistical analysis was performed using one-way analysis of variance followed by Bonferroni's post hoc test and false discovery rate (FDR) correction for multiple testing. \*\*p<0.01; \*\*\*p<0.001; \*\*\*\*p<0.0001; ns, not statistically significant.

only HSM and H1 improved insulin sensitivity in the insulin tolerance test (see online supplementary figure S5E, F).

HSM and H1 reduced serum levels of the pro-inflammatory cytokines IL-1 $\beta$  and TNF- $\alpha$ , compared with HFD (figure 1G,H). Consistent with the effects described above on lipid metabolism (see online supplementary figure S4), HSM and H1 reduced adipocyte hypertrophy and the number of crown-like structures (CLS)—tissue lesions in which macrophages surround dead adipocytes (see online supplementary figure S6). We monitored expression of mitochondrial uncoupling protein 1 (UCP1), which was identified earlier as a major regulator of thermogenesis in adipose tissues.<sup>40</sup> HSM and H1 increased UCP1 mRNA and protein expression in brown adipose tissues (BATs) and inguinal white adipose tissues (iWATs) compared with the HFD group (see online supplementary figure S7), suggesting that HSM and H1 may increase thermogenesis. Furthermore, HSM and H1 reduced signs of NAFLD and NASH, including liver cell hypertrophy and accumulation of lipid droplets, in the liver of HFD-fed mice (see online supplementary figure S8 and supplementary dataset S1). While HSM and H1 produced a modest but statistically significant reduction of body weight in chow-fed mice, the treatments did not affect visceral fat weight, HOMA-IR index or pro-inflammatory cytokine levels in this group (see online supplementary figure S9). These results indicate

that HSM and H1 produce anti-obesogenic, antidiabetic and anti-inflammatory effects in HFD-fed mice.

### HSM and H1 prevent leaky gut and metabolic endotoxemia

Previous studies have shown that an HFD reduces expression of intestinal tight junction proteins (eg, zonula occludens-1 (ZO-1)) and disrupts gut barrier integrity, leading to translocation of bacterial LPS into the blood (ie, metabolic endotoxemia) and producing inflammation and insulin resistance.<sup>5–7 15 41</sup> Notably, HSM and H1 significantly reduced serum endotoxin levels (figure 2A) and intestinal permeability (figure 2B) in HFD-fed mice. These observations were accompanied by increased expression of ZO-1 (figure 2C) and reduced mRNA expression of pro-inflammatory cytokines (figure 2D,E) in the colon of mice treated with HSM or H1. In contrast, fractions H2–H4 failed to reverse serum endotoxemia (figure 2A), intestinal permeability (figure 2B) or expression of colonic pro-inflammatory cytokines or ZO-1 (figure 2C–E). HSM and H1 significantly increased levels of regulatory T cells expressing the anti-inflammatory cytokine IL-10 in colonic lamina propria of HFD-fed mice (figure 2F), while reducing levels of M1 macrophages expressing pro-inflammatory IL-1 $\beta$  (figure 2G). In addition, H1 reduced LPS-induced disruption of cell monolayers (figure 2H, measured using the TEER assay)



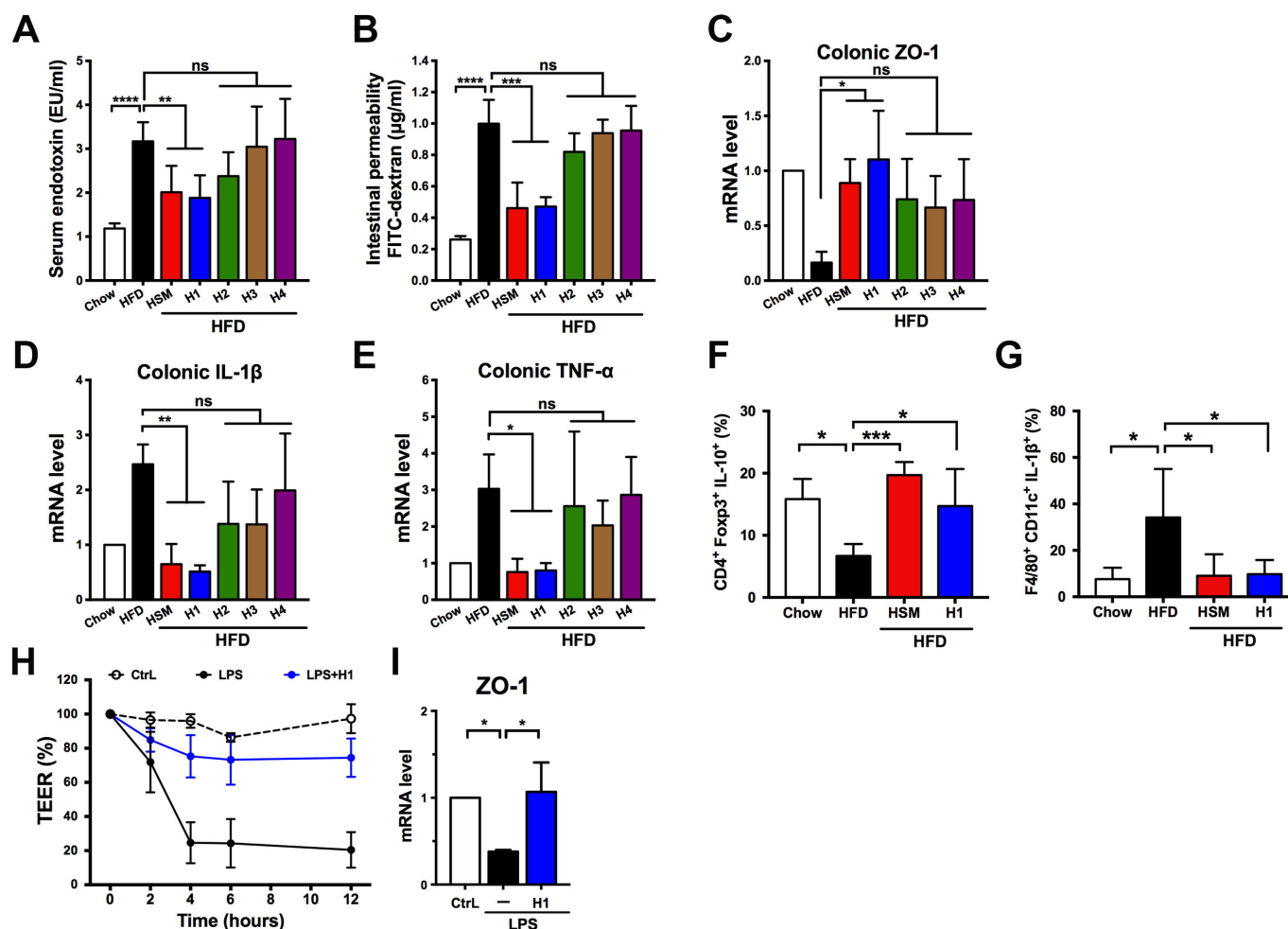


**Figure 2** *Hirsutella sinensis* mycelium (HSM) and H1 improve intestinal integrity and produce immunomodulatory effects. Experiments were performed as in figure 1. (A) Serum endotoxin and (B) intestinal permeability were measured as described in the 'Methods' section. (C) Zonula occludens-1 (ZO-1), (D) interleukin (IL)-1 $\beta$  and (E) tumour necrosis factor- $\alpha$  (TNF- $\alpha$ ) expression in proximal colon was examined using quantitative real-time PCR (qRT-PCR). Expression levels were normalised to glyceraldehyde 3-phosphate dehydrogenase and expressed as relative fold changes compared with the chow group. Levels of (F) IL-10-expressing regulatory T cells and (G) IL-1 $\beta$ -expressing M1 macrophages were analysed using flow cytometry. (H) In vitro Caco-2 cell permeability was monitored using the transepithelial electrical resistance (TEER) assay. (I) ZO-1 expression in Caco-2 cells was examined using qRT-PCR. Caco-2 cells were treated with control (Ctrl) serum-free medium, lipopolysaccharide (LPS) or LPS plus H1 for 12 hours. Expression levels were normalised to 18S rRNA and expressed as relative fold changes compared with the vehicle control. Data are presented as means $\pm$ SD from three independent experiments (A, B, n=10–15 mice/group; H, I, duplicate/group) or two independent experiments (C–G; n=5–10 mice per group). Statistical analysis was performed using one-way analysis of variance followed by Bonferroni's post hoc test and false discovery rate correction for multiple testing. \*P<0.05; \*\*p<0.01; \*\*\*p<0.001; \*\*\*\*p<0.0001; ns, not significant. FITC, fluorescein-isothiocyanate.

and increased ZO-1 mRNA expression (figure 2I) in colonic Caco-2 cells.

### The anti-obesogenic effects of HSM and H1 are transferable by faecal transplantation

The gut microbiota contributes to the development of diet-induced obesity and associated metabolic disorders.<sup>12–15</sup> Given that HSM and H1 reduced serum endotoxemia and intestinal permeability (figure 2A,B), we examined whether the beneficial effects of HSM and H1 may be mediated by the gut microbiota. Faecal microbiota from HFD-fed or chow-fed mice treated with saline, HSM, fraction H1 or fraction H4 were transplanted into HFD-fed recipients (see online supplementary figure S10A). FMT from HSM-treated, H1-treated or chow-treated mice reduced body weight gain and obesity traits in HFD recipients (see online supplementary figure S10B–G,I). FMT from

HSM, H1 or chow groups increased colonic ZO-1 mRNA expression compared with the controls (see online supplementary figure S10H). Furthermore, FMT from HSM, H1 or chow groups reduced adipocyte hypertrophy and CLS lesions (see online supplementary figure S11), as well as signs of NAFLD and NASH in the liver of HFD recipients (see online supplementary figure S12). In contrast, FMT derived from saline-treated or H4-treated, HFD-fed mice failed to reverse obesity traits in HFD-fed recipients (see online supplementary figures S10–12). These results suggest that the gut microbiota mediates the anti-obesogenic effects produced by HSM and H1.

### Neomycin abolishes H1's anti-obesogenic effects

To determine whether the anti-obesogenic effects of H1 are dependent on the presence of specific gut bacteria, we treated H1-fed HFD mice with a cocktail of antibiotics, which included

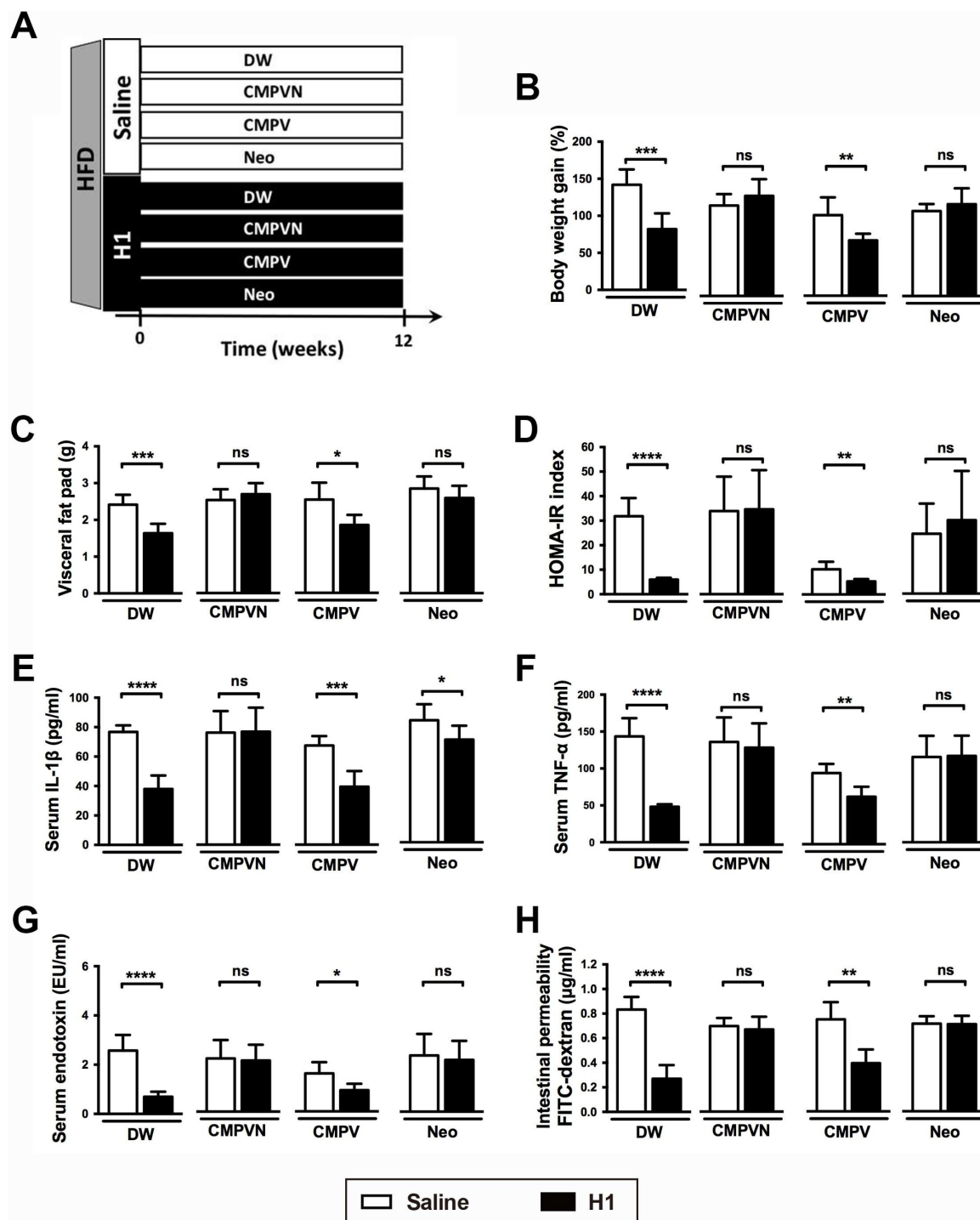


**Figure 3** H1 produces anti-obesogenic effects via neomycin-sensitive gut bacteria. (A) Saline-treated or H1-treated high-fat diet (HFD)-fed mice were treated orally with antibiotics in sterile drinking water (DW) for 12 weeks as described in the 'Methods' section. Obesity traits including (B) body weight gain, (C) visceral fat pad weight, (D) homeostatic model assessment-insulin resistance (HOMA-IR) index, (E) serum interleukin (IL)-1 $\beta$ , (F) serum tumour necrosis factor- $\alpha$  (TNF- $\alpha$ ), (G) serum endotoxin (lipopolysaccharide (LPS)) and (H) intestinal permeability were measured after 12 weeks of treatment. Data are presented as means $\pm$ SD ( $n=6$  mice/group). Statistical analysis was performed using unpaired Student's *t*-test between saline and H1 groups, followed by false discovery rate correction for multiple testing. \* $P<0.05$ ; \*\* $p<0.01$ ; \*\*\* $p<0.001$ ; \*\*\*\* $p<0.0001$ ; C, clindamycin; FITC, fluorescein-isothiocyanate; M, metronidazole; P, penicillin; V, vancomycin; N or Neo, neomycin; ns, not significant.

clindamycin (C), metronidazole (M), penicillin (P), vancomycin (V) and neomycin (N) in DW (figure 3A). Compared with the antibiotic-free DW control group in which H1 reduced body weight gain and obesity traits (figure 3B–H and supplementary figures S13–15, DW control group), treatment with the CMPVN antibiotic cocktail abolished H1's anti-obesogenic effects

(figure 3B–H and supplementary figures S14 and 15, CMPVN treatment).

To determine whether a single antibiotic from the cocktail may be responsible for these effects, we treated mice with individual antibiotics (see online supplementary figure S13A). Of note, with the exception of serum IL-1 $\beta$  (figure 3E), neomycin consistently

abrogated H1's anti-obesogenic effects (figure 3B–H, supplementary figure S13B–G and supplementary figures S14 and 15, Neo treatment), whereas, with few exceptions, the other single antibiotic treatments failed to block H1's effects (see online supplementary figure S13B–G). Furthermore, H1's anti-obesogenic effects were not affected by an antibiotic cocktail lacking neomycin (figure 3B–H and supplementary figures S14 and 15, CMPV treatment). Neomycin-sensitive gut bacteria may therefore be required for H1's anti-obesogenic effects.

### Identification of neomycin-sensitive gut bacteria enriched by H1

We used next-generation 16S rDNA sequencing to analyse the changes produced by H1 in the gut microbiota. Sequencing analysis of caecal samples (figure 4A) produced an average of  $117\,633 \pm 13\,834$  effective reads per sample that covered rare new phylotypes and broad bacterial diversity (see online supplementary dataset S2). Weighted UniFrac-based principal coordinate analysis revealed distinct clustering of microbiota for each group (see online supplementary figure S16A). Pairwise comparisons using the permutational multivariate analysis of variance (PERMANOVA) test indicated a statistically significant separation between groups ( $p < 0.05$ ), except for the comparison between CMPVN and CMPV ( $p = 0.41$ ). Analysis of distance matrix revealed that the gut microbiota of neomycin-treated mice clustered with that of HFD-fed mice (see online supplementary figure S16B), revealing similarities between the microbiota of these samples.

We used Metastats analysis to identify the bacteria altered by H1 and neomycin in HFD-fed mice. Operational taxonomic units showing a significant difference between H1 and the other HFD groups were searched against the GenBank sequence database. Overall, 40 bacterial species were significantly altered by H1 in HFD or antibiotics-treated mice (figure 4B,C and supplementary dataset S3). When compared with HFD, H1 altered 16 bacterial species (figure 4B,C; H1 vs HFD, 11 increased species highlighted in red and five reduced species highlighted in green in figure 4C; see also supplementary dataset S3). In H1-treated HFD groups, supplementation with CMPV, neomycin or CMPVN, respectively altered 19, 25 or 27 bacterial species (figure 4B,C; species highlighted in red or green in figure 4C). The chow treatment only affected the levels of nine bacterial species compared with HFD (figure 4B,C; chow vs HFD), indicating that H1 modulates the gut microbiota in a specific manner.

We sought to identify the bacterial species in the H1 group whose abundance was altered by both neomycin and CMPVN. Detailed analysis showed that, among the 40 bacterial species identified, 9 species were modulated in the same direction by both neomycin and CMPVN (figure 4B,C and supplementary dataset S3), including 6 species whose levels were enriched by H1 (*P. goldsteinii*, *Flintibacter butyricus*, *Intestinimonas butyriciproducens*, *Clostridium cocleatum*, *Clostridium viride* and *Anaerotruncus colihominis*) and 3 species whose levels were reduced by H1 (*Pseudomonas aeruginosa*, *Escherichia coli* and *Shewanella algae*). In contrast, three enriched species (*Ruminococcus flavefaciens*, *Butyrivibrio hungatei* and *Ruminococcus bromii*) and three depleted species (*Mucispirillum schaedleri*, *Dorea longicatena* and *Romboutsia timonensis*) were significantly modulated by H1 but reversed by neomycin treatment. Species whose levels were enriched by H1 but reduced by CMPVN included *Ruminococcus gnavus*, *Ochrobactrum anthropic* and *Delftia acidovorans*.

Among the altered species identified, *M. schaedleri*, *D. longicatena*, *R. timonensis*, *E. coli* and *S. algae* represent endotoxin-producing bacteria whose levels increased in obese animals.<sup>33 42 43</sup> Notably, several altered species, including *P. goldsteinii*, *C. cocleatum*, *A. colihominis* and *R. flavefaciens*, were reduced in obese animals and humans.<sup>33 44 45</sup> Our results showed that several bacterial species were altered in the same direction in the HFD group by CMPV, neomycin and CMPVN (figure 4C). Of note, the levels of four species, including *P. goldsteinii*, *I. butyriciproducens*, *C. cocleatum* and *S. algae*, were significantly altered by H1 but reversed by neomycin and CMPVN (figure 4C).

We examined whether obesity-related traits correlated with the levels of neomycin-sensitive gut bacteria enriched by H1. Spearman's correlation analysis showed that the levels of these bacteria negatively correlated with obesity traits (figure 4D). Notably, among these bacteria, *P. goldsteinii* was highly enriched by H1 treatment (figure 4B,C and supplementary dataset S3) and this species negatively correlated with all obesity traits (figure 4D and supplementary dataset S4). The levels of other H1-modulated neomycin-sensitive bacteria were also associated with *P. goldsteinii* levels (see online supplementary figure S17). These results suggest that *P. goldsteinii* and the neomycin-sensitive gut microbiota might mediate the anti-obesogenic effects of H1.

### Ex vivo neomycin treatment abolishes the anti-obesogenic effects of H1

To eliminate potential side effects produced by antibiotics on the host, we treated faecal microbiota with antibiotics ex vivo prior to FMT (ex-FMT; figure 5A). Faecal microbiota specimens collected daily from H1-treated HFD-fed mice were incubated with antibiotics or saline, followed by washing steps and oral administration into HFD-fed recipients (figure 5A). As expected, the HFD-induced obesity traits of HFD recipients were significantly reduced by ex-FMT from H1-treated mice (figure 5B–H, H1 vs HFD), and these effects were abolished by ex-FMT from neomycin-treated or CMPVN-treated animals (figure 5B–H). In contrast, ex-FMT from CMPV-treated H1-faecal microbiota prevented obesity traits in HFD animals (figure 5B–H, CMPV).

### *P. goldsteinii* levels negatively correlate with obesity traits in ex vivo FMT

We analysed the microbiota of ex-FMT mice to identify bacteria that were enriched by H1 but reduced by neomycin or CMPVN in donor and recipient mice. In the donor group, when compared with HFD, levels of eight bacterial species were significantly altered by H1 but reversed by neomycin and CMPVN (figure 6A,B and supplementary dataset S5). These bacteria included six species whose levels were enriched by H1 (*P. goldsteinii*, *Clostridium perfringens*, *C. viride*, *Adlercreutzia equolifaciens*, *Paenibacillus glucanolyticus* and *Bradyrhizobium japonicum*) and two species whose levels were reduced by H1 (*Lactobacillus johnsonii* and *Lactobacillus reuteri*; figure 6A,B and supplementary dataset S5). Among these bacteria, *P. goldsteinii* was significantly enriched in H1 donor mice but considerably reduced by neomycin or CMPVN (figure 6A,B). Accordingly, *P. goldsteinii* was also enriched in H1-recipient mice but reduced in CMPVN-recipient mice (figure 6C,D and supplementary dataset S6). Based on quantitative PCR, we observed that the absolute *P. goldsteinii* count increased following H1 treatment but the bacterial count was considerably reduced by neomycin or CMPVN in both donor and recipient mice (figure 6E). Notably,



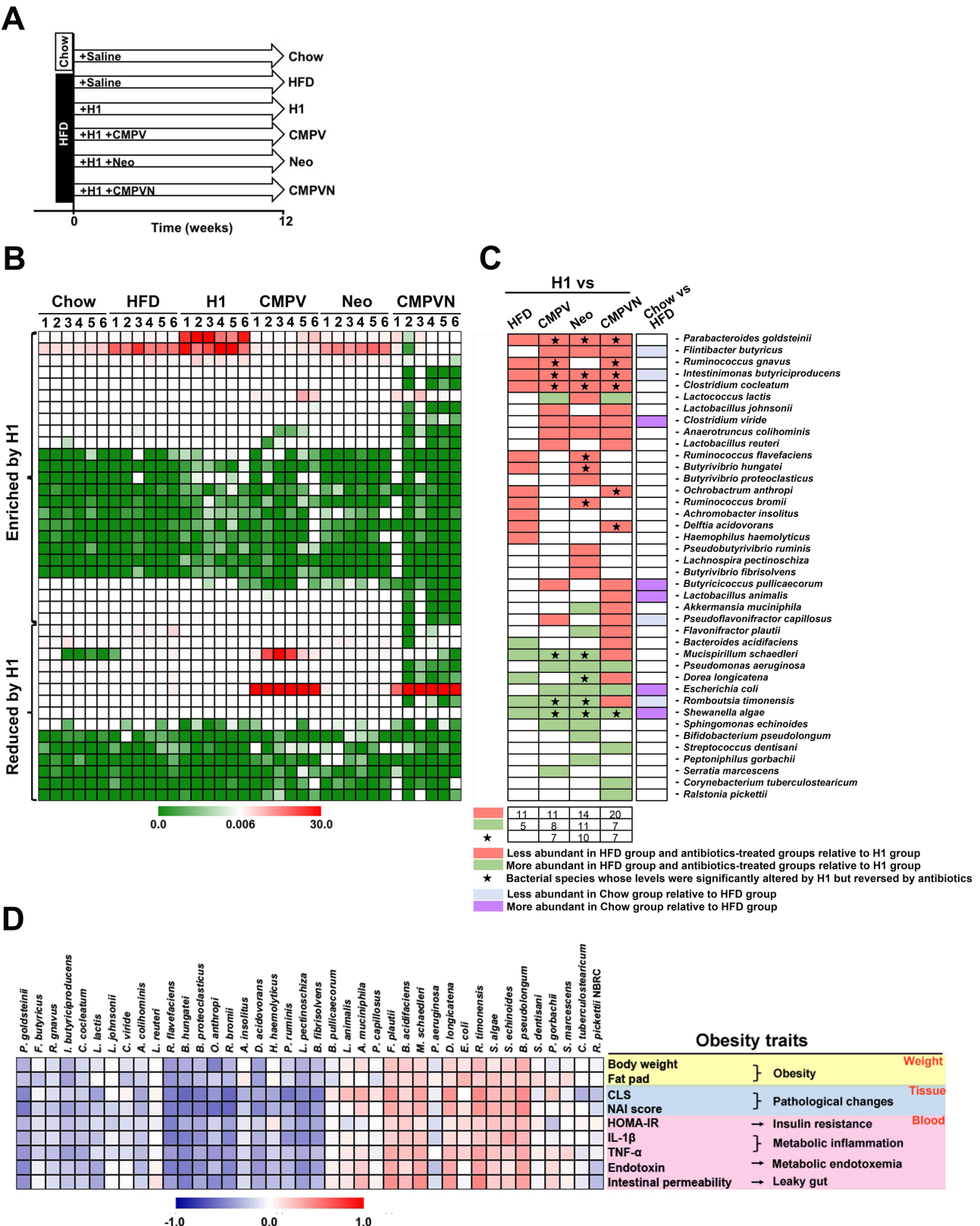


**Figure 4** H1 enriches a population of neomycin-sensitive gut bacteria that negatively correlates with obesity traits. (A) Mice were treated for 12 weeks as indicated. (B) Heatmap showing the levels of 40 bacterial species significantly altered by high-fat diet (HFD) or antibiotics in comparison with the H1 group based on Metastats analysis. (C) Bacterial species from panel B and changes induced by the treatments indicated. Green and red entries indicate species that were respectively more and less abundant in the HFD group and antibiotics-treated groups relative to H1. Purple and blue entries indicate species that were respectively more and less abundant in the chow group relative to the HFD group. Black stars indicate bacterial species whose levels were significantly altered by H1 but reversed by antibiotics. (D) Spearman's correlation analysis between the 40 identified bacterial species and obesity traits. False discovery rate correction for multiple testing was used. CLS, crown-like structure; HOMA-IR, homeostatic model assessment-insulin resistance; IL, interleukin; NAI, non-alcoholic steatohepatitis activity index; TNF- $\alpha$ , tumour necrosis factor-alpha.

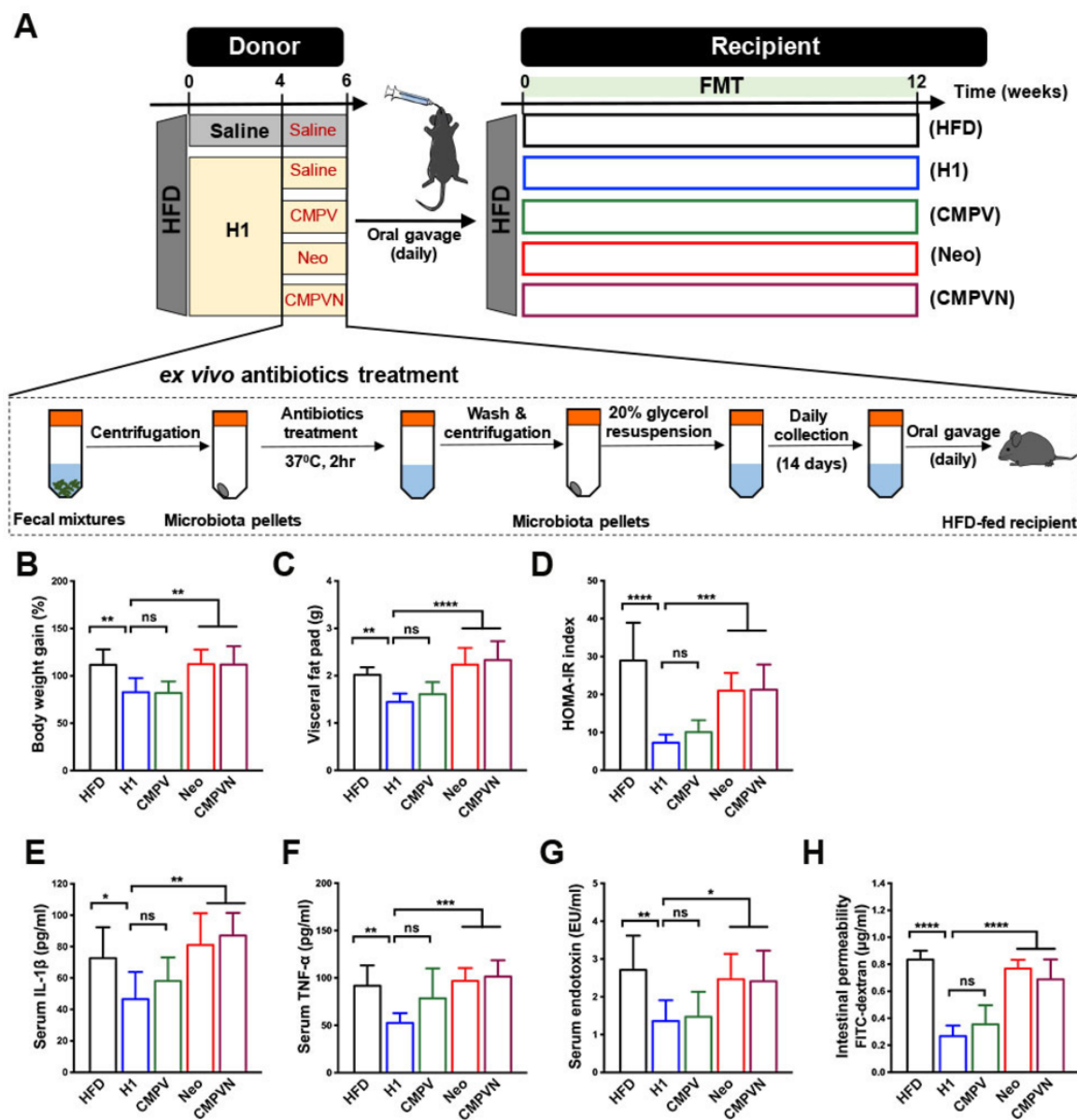


**Figure 5** Ex vivo neomycin treatment abolishes the anti-obesogenic effects of faecal microbiota transplantation (FMT) from H1-treated mice. (A) Diagram of ex vivo antibiotics treatment of faecal bacteria before FMT (ex-FMT). High-fat diet (HFD)-fed donor mice were treated daily with saline or H1 by oral gavage for 6 weeks. H1-treated faeces samples were collected daily from week 4 to 6, followed by a series of steps for ex vivo antibiotics treatment (CMPV, Neo, CMPVN or saline; see the enlarged rectangle). Faecal microbiota from saline-treated HFD-fed mice was used as a negative control. Faecal microbiota samples collected for 2 weeks from each donor mice were pooled and an equal volume was transferred to HFD-fed mice by oral gavage for 12 weeks. Obesity traits measured in recipients after 12 weeks included (B) body weight gain, (C) visceral fat pad weight, (D) homeostatic model assessment-insulin resistance (HOMA-IR) index, (E) serum interleukin (IL)-1 $\beta$ , (F) serum tumour necrosis factor- $\alpha$  (TNF- $\alpha$ ), (G) serum endotoxin and (H) intestinal permeability. Data are presented as means $\pm$ SD from two independent experiments (n=9). Data were analysed using one-way analysis of variance followed by Bonferroni's post hoc test and false discovery rate correction for multiple testing. \* $P$ <0.05; \*\* $P$ <0.01; \*\*\* $P$ <0.001; \*\*\*\* $P$ <0.0001; ns, not significant; FITC, fluorescein-isothiocyanate.

both the absolute count (copy number) and relative level of *P. goldsteinii* were negatively associated with obesity traits (figure 6F).

#### *P. goldsteinii* prevents diet-induced obesity and metabolic disorders

In order to confirm that *P. goldsteinii* had colonised mice in FMT experiments, we examined the levels of *P. goldsteinii* in caecal microbiota of HFD-fed mice treated with saline, HSM or H1 as well as in their recipients. Levels of *P. goldsteinii* between paired

donors and recipients were similar (see online supplementary figure S18A,B), indicating an efficient transfer of *P. goldsteinii* during FMT. Moreover, colonisation was observed in HFD-fed mice treated with neomycin for 8 weeks and which received a single oral gavage of *P. goldsteinii* (see online supplementary figure S18C).

These results prompted us to examine whether *P. goldsteinii* produces anti-obesogenic effects in HFD-fed mice. We treated HFD-fed mice daily with a commercial strain of *P. goldsteinii* or saline for 8 weeks (figure 7A). *P. goldsteinii* treatment

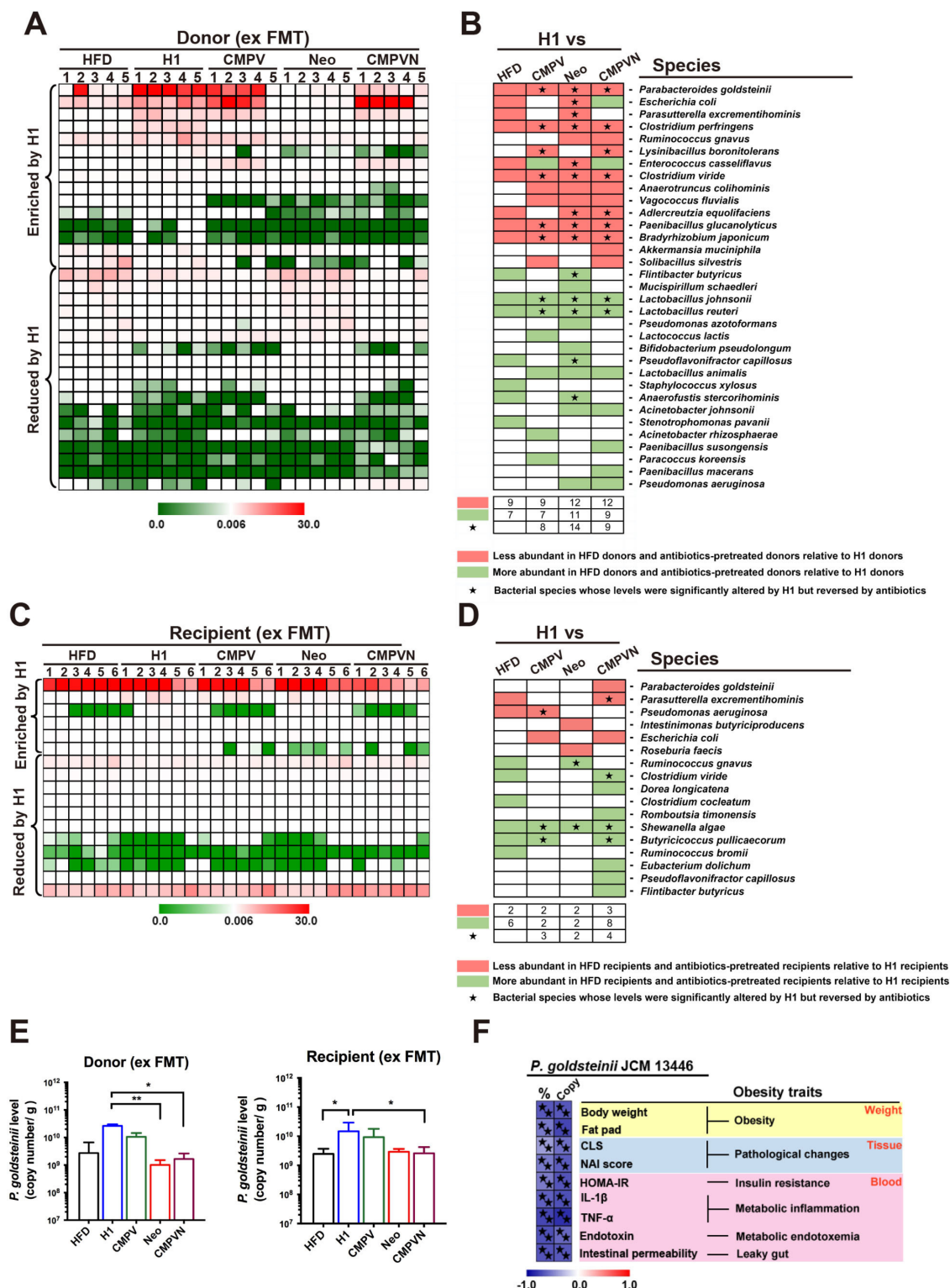


**Figure 6** *Parabacteroides goldsteinii* is enriched in ex vivo faecal microbiota transplantation (ex FMT) H1 donor and recipient mice and negatively correlates with obesity traits. The ex-FMT experiments are depicted in figure 5A. (A) Heatmap abundance and (B) bacterial species information showing 33 bacterial species significantly altered by H1 in donor groups based on Metastats analysis. (C) Heatmap abundance and (D) bacterial species information showing 17 bacterial species significantly altered by H1 in recipient groups based on Metastats analysis. In panels (B) and (D), green and red entries indicate species that were respectively more and less abundant in the high-fat diet (HFD) group and ex vivo antibiotics-treated groups relative to H1. Black stars indicate bacterial species whose levels were significantly altered by H1 but reversed by antibiotics. (E) Absolute quantification (copy number) of *P. goldsteinii* in ex-FMT donor groups (left panel) and recipient groups (right panel). Data are presented as medians±IQR (n=5 and n=6 for donor and recipient groups, respectively). (F) Spearman's correlation analysis of relative abundance (%) and absolute count (copy) of *P. goldsteinii* and obesity traits. In this panel, black stars indicate statistically significant difference based on Spearman's correlation analysis and false discovery rate correction (<5%). \*P<0.05; \*\*p<0.01; CLS, crown-like structures; HOMA-IR, homeostatic model assessment-insulin resistance; IL, interleukin; NAI, non-alcoholic steatohepatitis activity index; TNF-α, tumour necrosis factor-alpha.



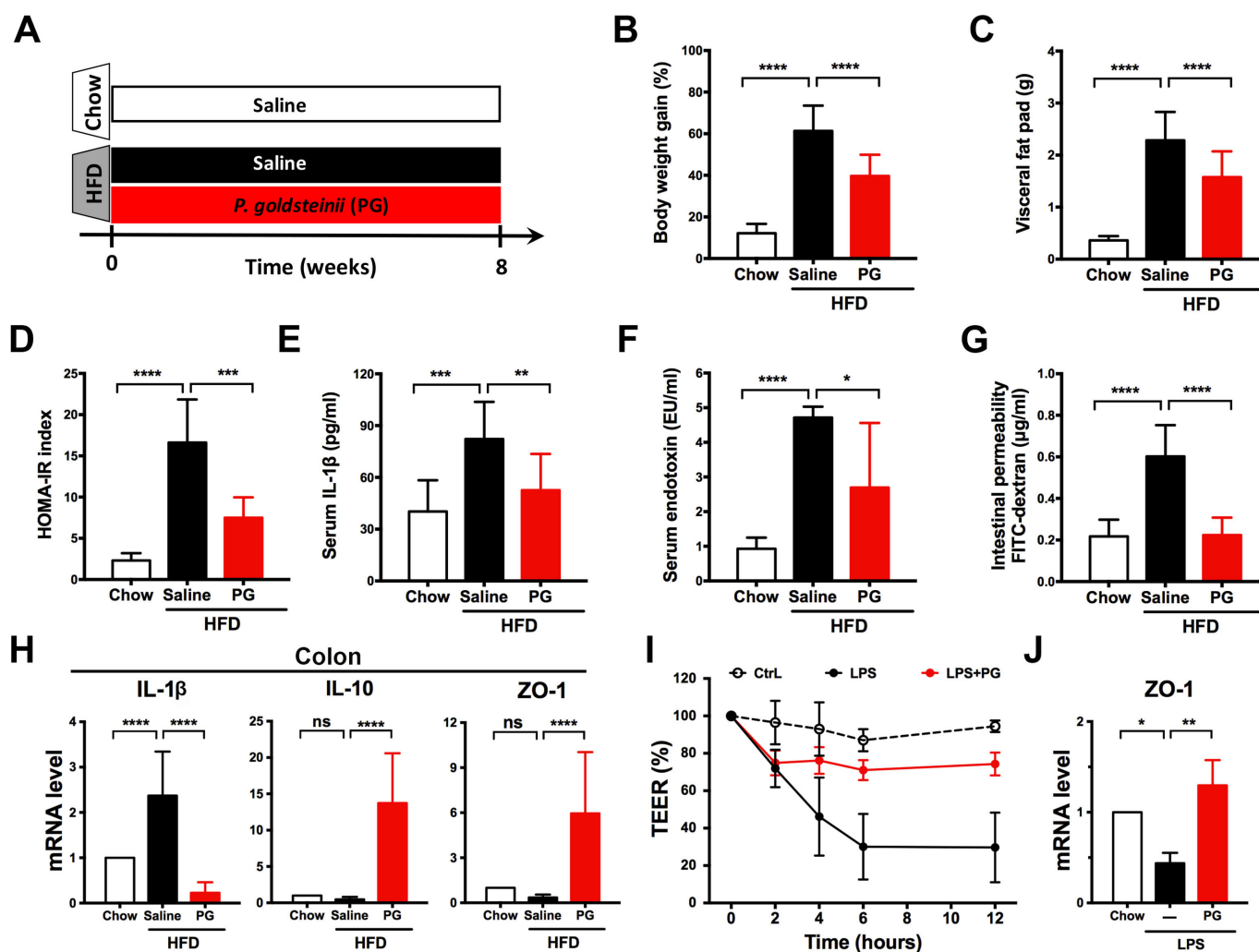


**Figure 7** *Parabacteroides goldsteinii* (PG) reduces diet-induced obesity and metabolic disorders. (A) Chow-fed mice and high-fat diet (HFD)-fed mice were treated daily with saline or PG ( $4 \times 10^7$  colony-forming units) by oral gavage for 8 weeks. Obesity traits including (B) body weight gain, (C) visceral fat pad, (D) homeostatic model assessment-insulin resistance (HOMA-IR) index, (E) serum interleukin (IL)-1 $\beta$ , (F) serum endotoxin and (G) intestinal permeability were measured after 8 weeks of treatment. (H) IL-1 $\beta$ , IL-10 and ZO-1 expression in proximal colon was examined using quantitative real-time PCR (qRT-PCR). Expression was normalised to glyceraldehyde 3-phosphate dehydrogenase and expressed as relative fold changes compared with the chow group. (I) Caco-2 cell permeability was monitored in vitro using the transepithelial electrical resistance (TEER) assay. (J) Zonula occludens-1 (ZO-1) expression in Caco-2 cell monolayers was examined using qRT-PCR. Expression was normalised to 18S rRNA and expressed as relative fold changes compared with the vehicle control (Ctrl). Data are presented as means  $\pm$  SD of three independent experiments.  $n=16-19$  mice for panels B, C;  $n=6$  for panels D, F, G;  $n=11$  for panels E, H;  $n=3$  for panels I, J. Data were analysed using one-way analysis of variance followed by Bonferroni's post hoc test and false discovery rate correction for multiple testing. \* $P < 0.05$ ; \*\* $p < 0.01$ ; \*\*\* $p < 0.001$ ; \*\*\*\* $p < 0.0001$ ; ns, not significant.

significantly reduced body weight gain (20%–35% reduction), visceral fat, HOMA-IR index, serum levels of IL-1 $\beta$  and endotoxin and intestinal permeability (figure 7B–G), and these results were accompanied by reduced IL-1 $\beta$  mRNA expression and increased IL-10 and ZO-1 mRNA expression in colon tissues (figure 7H). *P. goldsteinii* treatment also effectively reduced cell monolayer disruption and restored tight junction ZO-1 expression in LPS-treated Caco-2 cell monolayers (figure 7I,J). In chow-fed mice, *P. goldsteinii* treatment reduced body weight, but did not affect other obesity-related traits (see online supplementary figure S19). *P. goldsteinii* treatment reduced adipocyte hypertrophy and CLS lesions in adipose tissues of HFD-fed mice (see online supplementary figure S20). *P. goldsteinii* significantly increased UCP1 mRNA and protein expression in BATs and iWATs (see online supplementary figure S21), suggesting

that the bacterium may induce thermogenesis. Furthermore, *P. goldsteinii* reduced signs of NAFLD and NASH in HFD-fed mice (see online supplementary figure S22), and normalised gene expression involved in lipid transport, lipogenesis and  $\beta$ -oxidation in the liver (see online supplementary figure S23, no statistically significant effect was noted for SREBP1c). Notably, administration of either heat-killed or pasteurised *P. goldsteinii* failed to reduce body weight or visceral fat accumulation (see online supplementary figure S24), indicating that live bacteria are required to induce anti-obesogenic effects. Finally, *P. goldsteinii* treatment did not affect liver or kidney functions in chow-fed or HFD-fed mice (see online supplementary table S2). *P. goldsteinii* therefore induces anti-obesogenic, anti-inflammatory and antidiabetic effects in obese animals.

## DISCUSSION

Although previous studies have shown that the medicinal fungus *O. sinensis* may lower blood glucose and lipid levels in type 2 diabetes in mice,<sup>46–49</sup> the possibility that this fungus may modulate the gut microbiota and reduce body weight in animals had not been examined. Our study shows that a water extract of the *H. sinensis* fungus (ie, HSM) and a fraction containing high-molecular weight polysaccharides (ie, fraction H1) reduce diet-induced obesity and metabolic disorders by modulating gut microbiota composition,

improving intestinal integrity and inducing thermogenesis. H1 treatment reverses HFD-induced gut dysbiosis and increases the level of *P. goldsteinii* and other neomycin-sensitive bacteria. Such changes in the composition of the gut microbiota in turn improve HFD-induced intestinal integrity and insulin sensitivity, and reduce metabolic endotoxemia, inflammation, fat deposition, adipose tissue pathology and the development of fatty liver disease (figure 8). We also observed that H1 reduced LPS-induced cellular permeability in human intestinal Caco-2 cells (figure 2H,I), indicating that

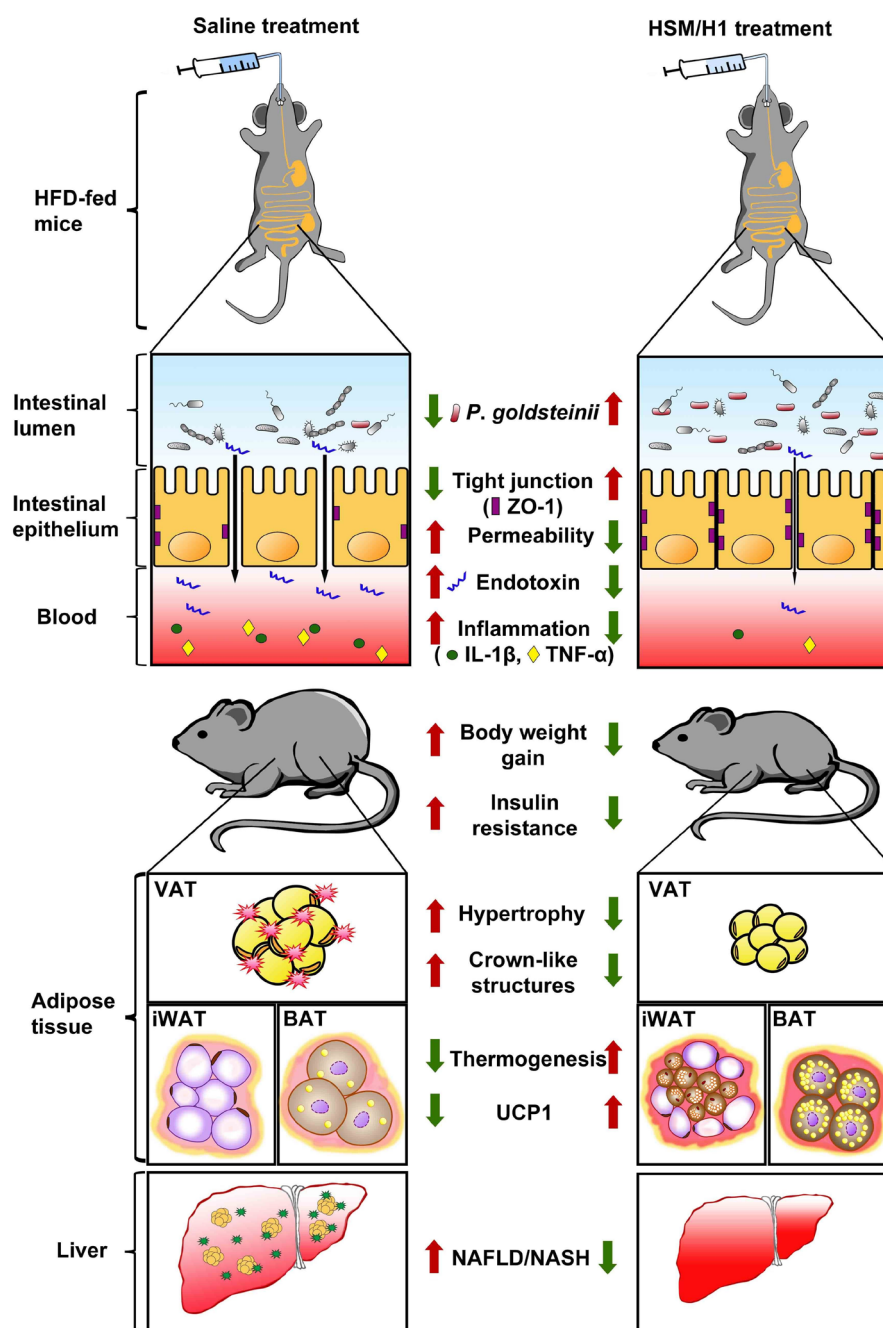


**Figure 8** Proposed model for the anti-obesogenic effects of *Hirsutella sinensis* mycelium (HSM) and H1 in high-fat diet (HFD)-fed mice. Treatment with HSM or H1 produces many beneficial changes on HFD-fed mice, including increasing *Parabacteroides goldsteinii* levels, tight junction expression and thermogenesis, while reducing gut permeability, blood endotoxin levels, inflammation and body weight. HSM and H1 also reduce insulin resistance, adipocyte hypertrophy, crown-like structures and signs of fatty liver disease (non-alcoholic fatty liver disease (NAFLD)/non-alcoholic steatohepatitis (NASH)). BAT, brown adipose tissue; IL, interleukin; iWAT, inguinal white adipose tissue; TNF- $\alpha$ , tumour necrosis factor-alpha; UCP1, uncoupling protein 1; VAT, visceral adipose tissue; ZO-1, zonula occludens-1.

H1 may improve intestinal integrity independently of the gut microbiota.

Our results show that *P. goldsteinii* treatment reduces obesity and metabolic disorders in HFD-fed mice, in addition to maintaining intestinal integrity, inducing thermogenesis and reducing endotoxemia and inflammation (figure 7A–H and supplementary figure S21). Intriguingly, a recent study showed that zwitterionic capsular polysaccharides derived from various commensal gut bacteria produce anti-inflammatory effects by inducing regulatory T cells.<sup>50</sup> Our observations that *P. goldsteinii* treatment induces expression of IL-10 (figure 7H) and helps maintain intestinal integrity (figure 7G,I,J) support the possibility that the bacterium may preserve intestinal homeostasis and improve gut barrier functions in vivo.

Our previous study showed that polysaccharides isolated from a water extract of the medicinal fungus *G. lucidum* also produce anti-obesogenic effects in HFD-fed mice.<sup>33</sup> Compared with the *G. lucidum* polysaccharides identified earlier, the monosaccharide composition of H1 identified here shows a higher content of mannose, galactose, N-galactosamine, N-glucosamine, rhamnose and fucose (see online supplementary table S3). Cordyceps polysaccharides have been found to contain  $\beta$ -glucans, heteroglycans and cordyglucans,<sup>29</sup> but the molecular structure and functional motifs of H1's high-molecular weight polysaccharides remain to be determined. While polysaccharides are predominantly enriched during water-based extraction procedures such as the one used to prepare the H1 fraction, we could not exclude the possibility that other bioactive molecules present in the extract may also contribute to the anti-obesogenic effects of this fraction. Moreover, we previously observed that *P. goldsteinii* levels in the gut microbiota of HFD-fed mice increased following treatment with *G. lucidum* polysaccharides,<sup>33</sup> suggesting that this commensal bacterial species may mediate the anti-obesogenic effects of polysaccharides isolated from various medicinal fungi.

The breakdown of polysaccharides and dietary fibre in mammals is mainly performed by intestinal bacteria, such as *Bacteroides thetaiotaomicron* and *Bacteroides fragilis*,<sup>51–54</sup> resulting in modulation of nutrient absorption and energy levels. HSM and H1 treatment did not alter energy intake, stool fat content or intestinal SCFA production (see online supplementary figures S2 and S3), indicating that the anti-obesity effects of H1 are not due to reduction of appetite, modulation of nutrient absorption or enhanced production of SCFAs. The reduction of *P. goldsteinii* levels by HFD and enrichment of this bacterial species by fungal polysaccharides indicate that the gut microbiota of polysaccharide-treated mice may contain higher levels of bacteria that preferentially metabolise polysaccharides. Enrichment of *P. goldsteinii* by H1 is also associated with reduced levels of bacterial species that are positively associated with obesity, such as *M. schaedleri* and *S. algae* (figure 4C).<sup>33 42 43 55</sup>

We observed that the anti-obesogenic effects of H1 are dependent on neomycin-sensitive gut bacteria (figures 3–6). The presence of a population of neomycin-sensitive gut bacteria and its association with obesity-related traits (figure 4D) suggests a potential beneficial interplay between these bacteria and energy regulation and metabolism. In the present study, H1 treatment did not affect the level of known commensal bacteria that possess anti-obesogenic properties, such as *A. muciniphila*,<sup>23 56</sup> *L. reuteri*<sup>57</sup> or *L. johnsonii*<sup>58</sup> (figure 4C). Further study of the functional gut microbiota and examination of their mechanism of action will be required to

identify new strategies to prevent and treat obesity and related metabolic disorders.<sup>59</sup>

Several medicinal fungi and plants produce beneficial effects on obesity and diabetes by modulating a variety of physiological pathways in the body.<sup>28</sup> In comparison to fractions H2 to H4, which produced small effects on a limited number of obesity traits (see for instance figure 1E and supplementary figure S4), HSM and fraction H1 produced consistent anti-obesogenic, antidiabetic and anti-inflammatory effects on all major obesity traits examined in HFD-fed mice, including HOMA-IR index (figure 1F), inflammation (figure 1G,H), metabolic endotoxemia (figure 2A) and intestinal permeability (figure 2B). Furthermore, besides reducing gene expression involved in lipogenic pathways in adipose and hepatic tissues (see online supplementary figure S4B,C), treatment with HSM and H1 significantly induced  $\beta$ -oxidation in the liver (see online supplementary figure S4C, *Acs13*). These results suggest that HSM and H1 may target specific metabolic and immunological pathways to normalise inflammatory markers and the metabolic profile of obese mice.

In conclusion, our results indicate that a water extract of a medicinal fungus and its high-molecular weight polysaccharide fraction reduce obesity, inflammation and diabetes-related symptoms by modulating the composition of the gut microbiota. Our findings show that both HSM and its high-molecular weight polysaccharides may be used as prebiotics—while the intestinal bacterium *P. goldsteinii* may be used as a probiotic—to prevent and treat obesity and the associated metabolic disorders.

#### Author affiliations

<sup>1</sup>Department of Medical Biotechnology and Laboratory Science, College of Medicine, Chang Gung University, Gueishan, Taiwan

<sup>2</sup>Graduate Institute of Biomedical Sciences, College of Medicine, Chang Gung University, Gueishan, Taiwan

<sup>3</sup>Center for Molecular and Clinical Immunology, Chang Gung University, Gueishan, Taiwan

<sup>4</sup>Microbiota Research Center, Chang Gung University, Gueishan, Taiwan

<sup>5</sup>Chang Gung Immunology Consortium, Linkou Chang Gung Memorial Hospital, Gueishan, Taiwan

<sup>6</sup>Research Center for Emerging Viral Infections, Chang Gung University, Gueishan, Taiwan

<sup>7</sup>Chang Gung Biotechnology Corporation, Taipei, Taiwan

<sup>8</sup>Biochemical Engineering Research Center, Ming Chi University of Technology, Taishan, Taiwan

<sup>9</sup>Department of Biomedical Sciences, University of the Pacific, Arthur Dugoni School of Dentistry, San Francisco, California, USA

<sup>10</sup>Department of Respiratory Therapy, Fu Jen Catholic University, Xinzhuang, Taiwan

<sup>11</sup>Laboratory of Cellular Physiology and Immunology, Rockefeller University, New York, USA

<sup>12</sup>Department of Laboratory Medicine, Linkou Chang Gung Memorial Hospital, Gueishan, Taiwan

<sup>13</sup>Research Center for Chinese Herbal Medicine, College of Human Ecology, Chang Gung University of Science and Technology, Gueishan, Taiwan

<sup>14</sup>Research Center for Food and Cosmetic Safety, College of Human Ecology, Chang Gung University of Science and Technology, Gueishan, Taiwan

**Acknowledgements** The authors would like to thank Dr Yu-Lun Kuo (Biotools) for the kind assistance with microbiota sequencing and analysis as well as Dr Yueh-Hsia Chiu (Chang Gung University) regarding the statistical analysis. The authors would also like to thank Drs Yu-Huan Tsai (Chang Gung University) and Julieta Schachter (Universidade Federal de Rio de Janeiro, Brazil) for their comments on the manuscript.

**Contributors** T-RW, C-SL and C-JC conceived the project, contributed to experimental design, performed experiments, interpreted the results, prepared the figures and wrote the manuscript; T-LL performed experiments and interpreted the results; JDY and H-CL conceived and supervised the project, interpreted the results and wrote the manuscript; JM, DMO and C-CL interpreted the results and wrote the manuscript; Y-FK provided the HSM extract and polysaccharides fractions; all authors discussed the results and approved the manuscript.



**Funding** The authors' work is supported by the Primordia Institute of New Sciences and Medicine; the Research Center for Emerging Viral Infections (Chang Gung University); the Featured Areas Research Center Program, which is part of the Higher Education Sprout Project of the Ministry of Education of Taiwan; by grants MOST105-2320-B-182-032-MY3, MOST105-2320-B-030-004, MOST103-2321-B-182-014-MY3 and MOST107-3017-F-182-001 from the Ministry of Science and Technology of Taiwan; and by grants BMRPA04, CMRPD1E0073, CMRPD1F0123, CORPD1F0011-3, QZRPD142 and QZRPD146 from Chang Gung Memorial Hospital.

**Competing interests** Y-FK is President of Chang Gung Biotechnology Corporation. JDY is Chairman of the Board of Chang Gung Biotechnology Corporation. The authors own patents related to the preparation and use of medicinal fungi and probiotics.

**Patient consent** Not required.

**Ethics approval** This study was approved by Chang Gung University's Institutional Animal Care and Use Committee (Document No. CGU11-117). Experiments were performed in accordance with the guidelines.

**Provenance and peer review** Not commissioned; externally peer reviewed.

## REFERENCES

- Caballero B. The global epidemic of obesity: an overview. *Epidemiol Rev* 2007;29:1–5.
- Haslam DW, James WP. Obesity. *Lancet* 2005;366:1197–209.
- World Health Organization. Obesity and overweight. 2018 <http://www.who.int/mediacentre/factsheets/fs311/en/>.
- Visscher TL, Seidell JC. The public health impact of obesity. *Annu Rev Public Health* 2001;22:355–75.
- Turnbaugh PJ, Ley RE, Mahowald MA, et al. An obesity-associated gut microbiome with increased capacity for energy harvest. *Nature* 2006;444:1027–131.
- Cani PD, Bibiloni R, Knauf C, et al. Changes in gut microbiota control metabolic endotoxemia-induced inflammation in high-fat diet-induced obesity and diabetes in mice. *Diabetes* 2008;57:1470–81.
- Cani PD, Possemiers S, Van de Wiele T, et al. Changes in gut microbiota control inflammation in obese mice through a mechanism involving GLP-2-driven improvement of gut permeability. *Gut* 2009;58:1091–103.
- Cani PD, Amar J, Iglesias MA, et al. Metabolic endotoxemia initiates obesity and insulin resistance. *Diabetes* 2007;56:1761–72.
- Hotamisligil GS. Inflammation and metabolic disorders. *Nature* 2006;444:860–7.
- Kennedy A, Martinez K, Chuang CC, et al. Saturated fatty acid-mediated inflammation and insulin resistance in adipose tissue: mechanisms of action and implications. *J Nutr* 2009;139:1–4.
- Morris DL, Cho KW, Delproposto JL, et al. Adipose tissue macrophages function as antigen-presenting cells and regulate adipose tissue CD4+ T cells in mice. *Diabetes* 2013;62:2762–72.
- Ridaura VK, Faith JJ, Rey FE, et al. Gut microbiota from twins discordant for obesity modulate metabolism in mice. *Science* 2013;341:1241214.
- Dethlefsen L, McFall-Ngai M, Relman DA. An ecological and evolutionary perspective on human-microbe mutualism and disease. *Nature* 2007;449:811–8.
- Yoshimoto S, Loo TM, Atarashi K, et al. Obesity-induced gut microbial metabolite promotes liver cancer through senescence secretome. *Nature* 2013;499:97–101.
- Hersoug LG, Møller P, Loft S. Gut microbiota-derived lipopolysaccharide uptake and trafficking to adipose tissue: implications for inflammation and obesity. *Obes Rev* 2016;17:297–312.
- Aguirre M, Venema K. The art of targeting gut microbiota for tackling human obesity. *Genes Nutr* 2015;10:472.
- Anand G, Zarrinpar A, Loomba R. Targeting Dysbiosis for the Treatment of Liver Disease. *Semin Liver Dis* 2016;36:037–47.
- Delzenne NM, Cani PD, Everard A, et al. Gut microorganisms as promising targets for the management of type 2 diabetes. *Diabetologia* 2015;58:2206–17.
- Scott KP, Antoine JM, Midtvedt T, et al. Manipulating the gut microbiota to maintain health and treat disease. *Microb Ecol Health Dis* 2015;26:25877.
- Sonnenburg JL, Bäckhed F. Diet-microbiota interactions as moderators of human metabolism. *Nature* 2016;535:56–64.
- Delzenne NM, Neyrinck AM, Bäckhed F, et al. Targeting gut microbiota in obesity: effects of prebiotics and probiotics. *Nat Rev Endocrinol* 2011;7:639–46.
- Everard A, Lazarevic V, Derrien M, et al. Responses of gut microbiota and glucose and lipid metabolism to prebiotics in genetic obese and diet-induced leptin-resistant mice. *Diabetes* 2011;60:2775–86.
- Everard A, Belzer C, Geurts L, et al. Cross-talk between *Akkermansia muciniphila* and intestinal epithelium controls diet-induced obesity. *Proc Natl Acad Sci U S A* 2013;110:9066–71.
- Wang J, Tang H, Zhang C, et al. Modulation of gut microbiota during probiotic-mediated attenuation of metabolic syndrome in high fat diet-fed mice. *Isme J* 2015;9:1–15.
- De Vadder F, Kovatcheva-Datchary P, Goncalves D, et al. Microbiota-generated metabolites promote metabolic benefits via gut-brain neural circuits. *Cell* 2014;156:84–96.
- Nakamura YK, Omaye ST. Metabolic diseases and pro- and prebiotics: Mechanistic insights. *Nutr Metab* 2012;9:60.
- Parnell JA, Reimer RA. Prebiotic fiber modulation of the gut microbiota improves risk factors for obesity and the metabolic syndrome. *Gut Microbes* 2012;3:29–34.
- Martel J, Ojcius DM, Chang CJ, et al. Anti-obesogenic and antidiabetic effects of plants and mushrooms. *Nat Rev Endocrinol* 2017;13:149–60.
- El Enshasy HA, Hatti-Kaul R. Mushroom immunomodulators: unique molecules with unlimited applications. *Trends Biotechnol* 2013;31:668–77.
- Wasser SP. Medicinal mushroom science: Current perspectives, advances, evidences, and challenges. *Biomed J* 2014;37:345–56.
- Martel J, Ko YF, Ojcius DM, et al. Immunomodulatory Properties of Plants and Mushrooms. *Trends Pharmacol Sci* 2017;38:967–81.
- Martel J, Ko YF, Liao JC, et al. Myths and Realities Surrounding the Mysterious Caterpillar Fungus. *Trends Biotechnol* 2017;35:1017–21.
- Chang CJ, Lin CS, Lu CC, Cc L, et al. *Ganoderma lucidum* reduces obesity in mice by modulating the composition of the gut microbiota. *Nat Commun* 2015;6:7489.
- Lo HC, Hsieh C, Lin FY, et al. A Systematic Review of the Mysterious Caterpillar Fungus *Ophiocordyceps sinensis* in Dong-ChongXiaCao (Dong Chong Xia Cao) and Related Bioactive Ingredients. *J Tradit Complement Med* 2013;3:16–32.
- Zhu ZY, Liu XC, Fang XN, et al. Structural characterization and anti-tumor activity of polysaccharide produced by *Hirsutella sinensis*. *Int J Biol Macromol* 2016;82:959–66.
- Ko YF, Liao JC, Lee CS, et al. Isolation, Culture and Characterization of *Hirsutella sinensis* Mycelium from Caterpillar Fungus Fruiting Body. *PLoS One* 2017;12:e0168734.
- Wang CY, Liao JK. A mouse model of diet-induced obesity and insulin resistance. *Methods Mol Biol* 2012;821:421–33.
- White JR, Nagarajan N, Pop M. Statistical methods for detecting differentially abundant features in clinical metagenomic samples. *PLoS Comput Biol* 2009;5:e1000352.
- Benjamini Y, Krieger AM, Yekutieli D. Adaptive linear step-up procedures that control the false discovery rate. *Biometrika* 2006;93:491–507.
- Shabalina IG, Petrovic N, de Jong JM, et al. UCP1 in brite/beige adipose tissue mitochondria is functionally thermogenic. *Cell Rep* 2013;5:1196–203.
- Kim KA, Gu W, Lee IA, et al. High fat diet-induced gut microbiota exacerbates inflammation and obesity in mice via the TLR4 signaling pathway. *PLoS One* 2012;7:e47713.
- Johnson-Henry KC, Donato KA, Shen-Tu G, et al. *Lactobacillus rhamnosus* strain GG prevents enterohemorrhagic *Escherichia coli* O157:H7-induced changes in epithelial barrier function. *Infect Immun* 2008;76:1340–8.
- Chiu CM, Huang WC, Weng SL, et al. Systematic analysis of the association between gut flora and obesity through high-throughput sequencing and bioinformatics approaches. *Biomed Res Int* 2014;2014:1–10.
- Lee H, Ko G. Effect of metformin on metabolic improvement and gut microbiota. *Appl Environ Microbiol* 2014;80:5935–43.
- Clarke SF, Murphy EF, Nilaweera K, et al. The gut microbiota and its relationship to diet and obesity: new insights. *Gut Microbes* 2012;3:186–202.
- Kan WC, Wang HY, Chien CC, et al. Effects of Extract from Solid-State Fermented *Cordyceps sinensis* on Type 2 Diabetes Mellitus. *Evid Based Complement Alternat Med* 2012;2012:1–10.
- Koh JH, Kim JM, Chang UJ, et al. Hypocholesterolemic effect of hot-water extract from mycelia of *Cordyceps sinensis*. *Biol Pharm Bull* 2003;26:84–7.
- Li SP, Zhang GH, Zeng Q, et al. Hypoglycemic activity of polysaccharide, with antioxidation, isolated from cultured *Cordyceps* mycelia. *Phytomedicine* 2006;13:428–33.
- Shi B, Wang Z, Jin H, et al. Immunoregulatory *Cordyceps sinensis* increases regulatory T cells to Th17 cell ratio and delays diabetes in NOD mice. *Int Immunopharmacol* 2009;9:582–6.
- Neff CP, Rhodes ME, Arnolds KL, et al. Diverse Intestinal Bacteria Contain Putative Zwitterionic Capsular Polysaccharides with Anti-inflammatory Properties. *Cell Host Microbe* 2016;20:535–47.
- Krajmalnik-Brown R, Ilhan ZE, Kang DW, et al. Effects of gut microbes on nutrient absorption and energy regulation. *Nutr Clin Pract* 2012;27:201–14.
- Ravcheev DA, Godzik A, Osterman AL, et al. Polysaccharides utilization in human gut bacterium *Bacteroides thetaiotaomicron*: comparative genomics reconstruction of metabolic and regulatory networks. *BMC Genomics* 2013;14:873.
- Schwalm ND, Townsend GE, Groisman EA. Multiple Signals Govern Utilization of a Polysaccharide in the Gut Bacterium *Bacteroides thetaiotaomicron*. *MBio* 2016;7:e01342–16.
- Wexler HM. Bacteroides: the good, the bad, and the nitty-gritty. *Clin Microbiol Rev* 2007;20:593–621.
- Ravussin Y, Koren O, Spor A, et al. Responses of gut microbiota to diet composition and weight loss in lean and obese mice. *Obesity* 2012;20:738–47.
- Schneeberger M, Everard A, Gómez-Valadés AG, et al. *Akkermansia muciniphila* inversely correlates with the onset of inflammation, altered adipose tissue metabolism and metabolic disorders during obesity in mice. *Sci Rep* 2015;5:16643.
- Qiao Y, Sun J, Xia S, et al. Effects of different *Lactobacillus reuteri* on inflammatory and fat storage in high-fat diet-induced obesity mice model. *J Funct Foods* 2015;14:424–34.

- 58 Xin J, Zeng D, Wang H, *et al.* Preventing non-alcoholic fatty liver disease through *Lactobacillus johnsonii* BS15 by attenuating inflammation and mitochondrial injury and improving gut environment in obese mice. *Appl Microbiol Biotechnol* 2014;98:6817–29.
- 59 Pedersen HK, Gudmundsdottir V, Nielsen HB, *et al.* Human gut microbes impact host serum metabolome and insulin sensitivity. *Nature* 2016;535:376–81.